



PERGAMON

International Journal of Heat and Mass Transfer 000 (2000) 000–000

International Journal of  
**HEAT and MASS  
 TRANSFER**

www.elsevier.com/locate/ijhmt

## 2 Removing the marching breakdown of the boundary-layer 3 equations for mixed convection above a horizontal plate

4 Pierre-Yves Lagrée

5 *Laboratoire de Modélisation en Mécanique, U.M.R. 7607, Université Paris VI, Boîte 162, 4 place Jussieu, Paris 75005, France*

6 Received 8 February 1999; received in revised form 4 February 2000

### 7 Abstract

8 The thermal mixed convection boundary-layer flow over a flat horizontal cooled plate is revisited. It is shown that  
 9 this flow is very similar to the one taking place in a free convection hypersonic boundary layer (with a shock in  $x^{3/4}$ ): the  
 10 observed singular solutions which branch out may then be reinterpreted in the framework of “triple deck” theory. Two  
 11 salient structures emerge, one in double deck, if the buoyancy is very small, and the other one in single deck, if the  
 12 buoyancy is  $O(1)$ . These two structures are a reinterpretation of Steinrück’s [J. Fluid. Mech. 278 (1994) 251–265] results.  
 13 A numerical simulation of the unsteady boundary layer in the case of impulsively started and cooled plate is carried out.  
 14 It leads to the separation of the boundary layer as predicted by the triple deck theory. A region of reverse flow is  
 15 obtained which depends on the outflow boundary condition. © 2000 Elsevier Science Ltd. All rights reserved.  
 16

### 17 1. Introduction

18 Here we consider the mixed convection problem of an  
 19 incompressible buoyant (following the Boussinesq ap-  
 20 proximation) fluid flowing over a semi-infinite horizon-  
 21 tal flat plate at a constant temperature lower than the  
 22 incoming flow temperature (see Fig. 1 for a definition  
 23 sketch). Obviously, for a given  $x$  location, the fluid  
 24 temperature, by diffusion, increases from the wall value  
 25 towards that of the free stream. But for a fixed  $y$  loca-  
 26 tion, the convection induces a longitudinal decrease of  
 27 the temperature. The outcome is a buoyancy induced  
 28 streamwise adverse pressure gradient. This gradient  
 29 brakes the flow, and this creates an interaction between  
 30 the thermics and the dynamics. This mechanism of  
 31 mixed convection breakdown has been stated by  
 32 Schneider and Wasel [32] (other examples of re-com-  
 33 putation with different numerical methods are reviewed  
 34 by Steinrück [37]); they showed that this interaction  
 35 promotes a breakdown of the mixed boundary layer  
 36 equation: at a relatively small abscissa, the equations are  
 37 abruptly singular. Instead of a buoyant boundary layer,  
 38 a buoyant wall jet may be studied; the case of adiabatic

wall was studied by Daniels [10] and Daniels and 39  
 Gargaro [11], and they arrived at the same conclusions. 40  
 The wall jet problem is solved numerically and asymp- 41  
 totically by Higuera [17] who notes that the equations 42  
 are not parabolic as he noted before in the case of the 43  
 hydraulic jump, which is very similar in its behaviour. 44

To a certain extent, this self-induced braking may be 45  
 explained through a retroactive process involving inte- 46  
 gral concepts as follows: as the variation of pressure is 47  
 more or less proportional to the variation of the 48  
 boundary layer thickness (because of buoyancy;  $J$ , de- 49  
 fined by Eq. (1), will be the parameter), then the increase 50  
 of boundary layer thickness promotes a rise in pressure, 51  
 which decreases the velocity, and the result is an increase 52  
 of the boundary layer thickness; the process is self-pro- 53  
 moting. The failure of the integral method is presented 54  
 in Schneider and Wasel’s work [32]. Similar phenomena 55  
 were observed in interacting boundary layer flows and 56  
 described in [22,41] with a self-induced mechanism in- 57  
 volving variations of boundary layer thickness and 58  
 pressure (the difference being that in supersonic flows, 59  
 the variations of the slope of the boundary layer give rise 60  
 to pressure changes). The key mechanism in supersonic 61  
 and hypersonic flows was introduced by Neiland [25] 62  
 and Stewartson and Williams [43]: it is the “triple deck” 63  
 theory which clarifies the scales and the equations in- 64

*E-mail address:* pyl@ccr.jussieu.fr (P.-Y. Lagrée).

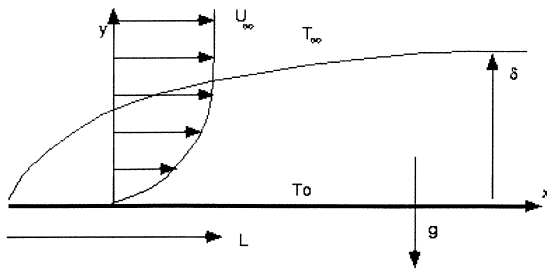


Fig. 1. Sketch of the mixed convection boundary layer flow. The temperature of the plate is different from the temperature of the flow. If the plate is cooled, the buoyancy induces an adverse pressure gradient.

show, at different scales (Section 3.2). In this case the overall process takes place in the thin wall layer itself and there is no retroaction from the main part of the boundary layer (this is similar to what happens in pipe flows: [29,33]). This structure is similar in a certain sense to Daniels [10] and to what Steinr ck [37] refers to as the “other large eigenvalues”. We next examine the above breakdown using integral methods (Section 4). A solution with a back flow valid after the singular point is exhibited and discussed; links with triple deck analysis are presented.

Finally (Section 5), we present a boundary layer calculation with a simple finite difference method of the complete problem. To avoid the preceding problems unsteadiness is introduced: the plate is impulsively heated and started. We will see that a good choice in discretizing the longitudinal derivative in the equations and a good choice of outflow conditions prevent the spatial singularity: this allows the boundary layer to separate with neither evidence of finite time breakdown [45] nor instabilities. The skin friction will be shown to be coherent with Steinr ck’s results [37], and each of his branched solutions may be interpreted as a solution of a domain of different length.

**2. Governing equations of the mixed convection** 129

*2.1. Equations* 130

We consider an incompressible two-dimensional flow past a semi-infinite (heated or cooled) horizontal flat plate (Fig. 1). The boundary layer equations are obtained from the Navier–Stokes counter parts subject to the Boussinesq approximation for a large Reynolds number. A re-scaling of the dimensional quantities is carried out with the dynamical boundary layer scales (with  $\delta = Re^{-1/2}$  with  $Re = \rho_\infty U_\infty L / \mu$ ):

$$u^* = U_\infty u, \quad v^* = \delta U_\infty v, \quad x^* = Lx, \quad y^* = \delta Ly, \\ p^* = p_\infty + \rho_\infty U_\infty^2 p, \quad T = T_\infty + (T_0 - T_\infty)\theta.$$

The result is the classical system (2)–(5) of thermal mixed convection [32]; Prandtl number is assumed to be of order unity and hence set (without to much loss of generality) to one while the Eckert number is assumed sufficiently small to obtain the energy equation as (5). The remaining parameter is the Richardson number or buoyancy parameter:

$$J = \frac{\alpha g (T_0 - T_\infty) L Re^{-1/2}}{U_\infty^2}, \tag{1}$$

which depends on  $\alpha$ , the thermal coefficient of expansion of the density in the Boussinesq approximation. The transverse pressure term (4) contains the gravity term, as

65 volved in the interaction. Brown, Stewartson and Wil-  
66 liams [7], and Brown and Stewartson [6] successfully  
67 explained the branching solutions calculated in strong  
68 hypersonic flows by Werle et al. [46] and the link with  
69 Neiland [25] (this is a free convection hypersonic  
70 boundary layer where the shock and the boundary layer  
71 behave in  $x^{3/4}$ ). Since both the mechanism of “thermal  
72 mixed convection with low wall temperature” and of the  
73 “strongly interacting hypersonic boundary layer” seem  
74 to follow qualitatively the same path, we propose to  
75 revisit the mixed convection with the triple deck tool (see  
76 [35] for other examples).

77 Thermal effects in boundary layer with triple deck  
78 have been already studied in the case of stratification in  
79 the upper deck by Sykes [44] and without buoyancy by  
80 Mendez et al. [24] or on a vertical plate by El Hafi [12].  
81 Some triple deck in mixed convection is in [19], and is  
82 extended herein.

83 In this paper we see (Section 3.1) that the result of the  
84 triple deck theory is that, in a mixed thermal linearized  
85 boundary layer (cold wall with very small buoyancy  $J$ ),  
86 there exist eigen solutions where pressure is proportional  
87 to the displacement of the streamlines; this is like the  
88 birth of a hydraulic jump [3,13,16] or a hypersonic  
89 boundary layer [7, 13]. In the case of a hot wall, pressure  
90 is proportional to the negative of the displacement of the  
91 streamlines in the main part of the boundary layer which  
92 leads to no upstream influence but this approach cap-  
93 tures the Tollmien Schlichting waves [34]. This triple  
94 deck result of strong self-induced upstream influence will  
95 be shown to be exactly the eigen function found by  
96 Steinr ck [37] but in the limit of small  $J$ . He showed that  
97 small perturbations from the solution at a given location  
98 (before the previously computed singularity) are ampli-  
99 fied exponentially; so the position of the singularity de-  
100 pends strongly on the amplification of the small  
101 numerical errors. If, thanks to a very refined calculation,  
102 the branching solutions are not selected, the buoyancy  
103 becomes greater and greater. If it is of order  $O(1)$ , a self-  
104 induced interaction is again possible, but, as we will

151 Eq. (4) holds for terms greater than  $O(1/Re)$ , we have  
 152  $|J| \gg Re^{-1}$ :

$$\frac{\partial}{\partial x} u + \frac{\partial}{\partial y} v = 0, \tag{2}$$

154

$$u \frac{\partial}{\partial x} u + v \frac{\partial}{\partial y} u = -\frac{\partial}{\partial x} p + \frac{\partial}{\partial y} \frac{\partial}{\partial y} u, \tag{3}$$

156

$$0 = -\frac{\partial}{\partial y} p + J\theta, \tag{4}$$

158

$$u \frac{\partial}{\partial x} \theta + v \frac{\partial}{\partial y} \theta = \frac{\partial}{\partial y} \frac{\partial}{\partial y} \theta. \tag{5}$$

160 Boundary conditions are:

$$u(x, y = 0) = 0, \quad v(x, y = 0) = 0, \tag{6}$$

162  $\theta(x, y = 0) = \theta_w$  with  $\theta_w = 1, \quad u(x, y \rightarrow \infty) = 1,$

163  $\theta(x, y \rightarrow \infty) = 0, \quad p(x, y \rightarrow \infty) = 0.$

164 2.2. *Marching breakdown*

165 In this work the length scale  $L$  and the parameter  $J$  are  
 166 independent, in contrast to the situation in [32] or in  
 167 [11]. In the “real mixed convection problem with stable  
 168 stratification flow”, the “natural” longitudinal scale is  
 169 effectively built with Richardson number. It is the length  
 170 that gives unit Richardson number ( $|xg(T_0 - T_\infty)$   
 171  $L_T U_\infty^{-2} (U_\infty L_T v^{-1})^{-1/2}| = 1$ ), so

$$L_T = \frac{U_\infty}{v} \left( \frac{U_\infty^2}{-xg(T_0 - T_\infty)} \right)^2.$$

173 Note that  $J^2 L_T = L$ . Schneider and Wasel [32] (scaled  
 174 with  $L_T$ ) showed that this system leads to a singularity  
 175 when solved with a marching (in increasing  $x$ ) resolu-  
 176 tion. They showed that the breakdown occurs for a  
 177 rather small abscissa. This is the reason why Steinrück  
 178 [37] (scaled with  $L_T$ ) has investigated how the system (2)–  
 179 (5) behaves when  $x$  tends to 0. In Fig. 2 are displayed,  
 180 with symbols, the reduced skin friction from previous  
 181 works compiled by Steinrück. The curves with numbers  
 182 show solution of the marching problem with slightly  
 183 perturbed initial conditions and come from his analysis  
 184 near  $x = 0$ . Asymptotic analysis suggests, however, that  
 185 it is better to consider an intermediate scale  $L$  (with  
 186  $L \ll L_T$ ) leading to Blasius boundary layer (with this  
 187 scale  $x$  tends to 0 is the nose effect) with a small thermal  
 188 perturbation gauged by  $|J| \ll 1$ , this means that the  
 189 Richardson number built with this abscissa is smaller  
 190 than one. So, we will introduce the triple deck analysis.

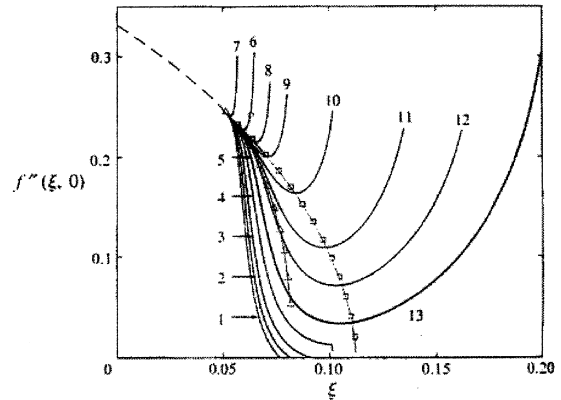


Fig. 2. The reduced skin friction compiled and computed by Steinrück (JFM 94). The numbered curves show solution of the marching problem with slightly perturbed initial conditions.

3. Asymptotic analysis: the triple deck tool

191

3.1. *Small J, with displacement*

192

3.1.1. *Main deck*

193

194 Here we look for eigen solutions in a boundary layer  
 195 slightly perturbed by the thermal effect in order to show  
 196 that system (2)–(5) is not parabolic in  $x$  when the plate is  
 197 cooled. We use the word “parabolic” for a system of  
 198 PDE in the sense of a system that can be integrated in  
 199 marching in  $x$  direction from upstream to downstream  
 200 (with no separation). The basic flow, driven by the free  
 201 stream uniform velocity, is a classical Blasius boundary  
 202 layer (thermal and dynamical effects are not coupled).  
 203 We study how a localized disturbance evolves at the  
 204 distance  $L$  downstream from the leading edge. At this  
 205 point, the boundary layer thickness is  $Re^{-1/2}L$ . Pure  
 206 thermal convection is relevant as long as the transverse  
 207 gradient from (4) is small which implies  $1 \gg |J|$ . So, in  
 208 this framework, the forced thermal boundary layer is of  
 209 the same thickness as the dynamic one, and the velocity  
 210 at station  $x = 1$  is the basic Blasius velocity profile (say  
 211  $U_0(y)$ , the transverse variable is then the same as the self-  
 212 similar one) and  $\theta$  is simply  $\theta_0(y) = 1 - U_0(y)$ . The  
 213 choice of  $L$  smaller than  $L_T$  suggests expanding in  
 214 powers of a small parameter  $\varepsilon$  linked to  $J$ .

215 Having defined the “basic state”, we follow the clas-  
 216 sical triple deck analysis [25,35,43], and more precisely  
 217 [20]: system (2)–(5) is re-investigated with a smaller  
 218 longitudinal scale, say  $x_3 L$  (with  $x_3 \ll 1$  and  $x = 1 + x_3 \bar{x}$ );  
 219 this scale is sufficiently small so that the preceding pro-  
 220 files may be considered as frozen. The reason for this  
 221 new scale is the fact that near the breakdown point the  
 222 gradient of the skin friction is infinite at scale 1, so we  
 223 hope to render it  $O(1)$  at this smaller scale. This layer  
 224 with height  $\delta L$  and length  $x_3 L$  is in fact the “main deck”.  
 225 Next we suppose that the perturbation of longitudinal

226 speed in the main deck is of the order of  $\varepsilon$  and the  
 227 pressure of the order of  $\varepsilon^2$ , where  $\varepsilon$  is unknown (but  
 228 depends on  $\delta, J$  and  $x_3$ ), so we recover at these scales the  
 229 inviscid problem with no longitudinal pressure gradient.  
 230 The perturbations are then linked by an up to now un-  
 231 known displacement function of the boundary layer  
 232 called  $-A(\bar{x})$  by Stewartson. In the main deck, the adi-  
 233 mensionalized velocities and temperature up to the order  
 234 of  $\varepsilon$  are:

$$u = U_0(y) + \varepsilon A(\bar{x})U'_0(y), \quad v = \frac{-\varepsilon A'(\bar{x})U_0(y)}{x_3},$$

$$\theta = \theta_0(y) + \varepsilon A(\bar{x})\theta'_0(y). \tag{7}$$

236 For the temperature, as for the speed, there is a  
 237 matching between the outer limit of the main deck and  
 238 the inner limit of the upper deck, and likewise for the  
 239 bottom of the main deck and the top of the lower deck  
 240 (those decks are defined later). We see that the temper-  
 241 ature behaves as the Stewartson  $S$  function (total enth-  
 242 alpy) in hypersonic flows ([6, 7, 26]). This perturbation  
 243 of temperature gives rise to a transverse change of  
 244 pressure through the main deck; we develop (4) in  
 245 powers of  $\varepsilon$  as follows:

$$\frac{\partial}{\partial y} p_0 + \varepsilon \frac{\partial}{\partial y} p_1 + \varepsilon^2 \frac{\partial}{\partial y} p_2 + O(\varepsilon^3)$$

$$= J(\theta_0(y) + \varepsilon A(\bar{x})\theta_0'(y)) + O(\varepsilon^3). \tag{8}$$

247 At this stage, for  $|J| \ll 1$  by minor degeneration (i.e. to  
 248 retain the maximum of terms), we put  $J = \varepsilon \tilde{J}$ , because  $J$   
 249 is small with  $\tilde{J}$  being a reduced Richardson number of  
 250 the order of  $O(1)$ . Looking at each power of  $\varepsilon$ , we see  
 251 that the first term is zero (as we supposed in the Blasius  
 252 Boundary layer); the second one shows that there is a  
 253 pressure stratification coming from basic temperature  
 254 profile ( $\int_0^\infty \theta_0(y) dy$ ), it does not depend on  $\bar{x}$  at the short  
 255 scale  $x_3$ , and it will appear that such a term can be ig-  
 256 nored in the following analysis; the third one integrates  
 257 (using  $\theta_0(\infty) = 0$ ;  $\theta_0(0) = 1$  by definition) as

$$p_2(\bar{x}, y \rightarrow \infty) - p_2(\bar{x}, y \rightarrow 0) = \tilde{J}A(\bar{x})(\theta_0(\infty) - \theta_0(0))$$

$$= -\tilde{J}A(\bar{x}),$$

259 where  $p_2(\bar{x}, y \rightarrow \infty)$  splices with upper deck and  
 260  $p_2(\bar{x}, y \rightarrow 0)$  with lower deck hitherto both being not  
 261 defined. The case  $J$  of the order of one will be discussed  
 262 later (Section 3.2), surprisingly, it implies again that  $p_1$   
 263 does not drive the flow in the main deck.

264 *3.1.2. Lower deck*

265 From solution (7), we see that the no-slip condition is  
 266 violated:  $u \rightarrow U'_0(0)(y + \varepsilon A)$ , and  $\theta \rightarrow \theta'_0(0)(y + \varepsilon A)$  as  
 267  $y \rightarrow 0$ . So we introduce a new layer of thickness  $\varepsilon$  (in  
 268 boundary layer scales), and scale  $y$  by  $\varepsilon \bar{y}$ , so the scale of  
 269  $u$  is  $\varepsilon \bar{u}$  and, by least degeneracy of Eq. (2), we have  
 270  $p = \varepsilon^2 \bar{p}$  (which is consistent with the matching

$\varepsilon^2 p_2(\bar{x}, y \rightarrow 0) = \varepsilon^2 \bar{p}(\bar{x}, \bar{y} \rightarrow \infty)$ ) and  $v$  is of the order of  
 $\varepsilon/x_3$ . The convective diffusive equilibrium gives the re-  
 lation between  $x_3$  and  $\varepsilon$ :  $x_3 = \varepsilon^3$ . The problem of mixed  
 convection near the wall is then:

$$\frac{\partial}{\partial \bar{x}} \bar{u} + \frac{\partial}{\partial \bar{y}} \bar{v} = 0, \tag{9}$$

$$\bar{u} \frac{\partial}{\partial \bar{x}} \bar{u} + \bar{v} \frac{\partial}{\partial \bar{y}} \bar{u} = -\frac{d}{d\bar{x}} \bar{p} + \frac{\partial}{\partial \bar{y}} \frac{\partial}{\partial \bar{y}} \bar{u}, \tag{10}$$

$$\bar{u} \frac{\partial}{\partial \bar{x}} \bar{\theta} + \bar{v} \frac{\partial}{\partial \bar{y}} \bar{\theta} = \frac{\partial}{\partial \bar{y}} \frac{\partial}{\partial \bar{y}} \bar{\theta}. \tag{11}$$

Boundary conditions are no-slip at the wall  
 $\bar{\theta}(\bar{x}, 0) = 1$ ,  $A(-\infty) = 0$ , and for  $\bar{y} \rightarrow \infty$ , the matchings:  
 $\bar{u} \rightarrow U'_0(0)(\bar{y} + A)$ ,  $\bar{p} \rightarrow p_2(\bar{x}, y \rightarrow 0)$  and  $\bar{\theta} \rightarrow 1 - U'_0(0)$   
 $(\bar{y} + A)$ . This set of non-linear equations is relevant in  
 the ‘‘lower deck’’ of length  $x_3 L = \varepsilon^3 L$  and of height  $\varepsilon \delta L$   
 placed at station 1; here, the thermal and the dynamical  
 problems are uncoupled. In this thin layer of small ex-  
 tent, the pressure coming from the main deck is the most  
 dangerous for the velocity and may lead to separation.

3.1.3. *The upper deck*

3.1.3.1. *Possibility of retroaction with the external flow.*

The perturbations of transverse velocity and pressure at  
 the edge of the main deck introduce a perturbation in  
 the inviscid flow: the upper deck is of size  $\varepsilon^3$  in both  
 directions. This perturbation is solved by the standard  
 technique of linearized subsonic perfect fluid, this gives  
 the Hilbert integral (the new pressure displacement re-  
 lation)

$$\frac{1}{\pi} \int \frac{-A'}{\bar{x} - \xi} d\xi - p_2(\bar{x}, y \rightarrow 0) = -\tilde{J}A(\bar{x})$$

and the usual gauge [35]:  $\varepsilon = \delta^{-1/4} = Re^{-1/8}$  (so  
 $J = Re^{-1/8} \tilde{J}$ ) and this gives the lower limit for  
 $x_3 = Re^{-3/8}$  in Section 3.1.2. The effect of the tempera-  
 ture is to add a new term proportional to the displace-  
 ment function  $A$ , it may be interpreted as a hydrostatic  
 pressure variation.

3.1.3.2. *Retroaction only in the boundary layer.*

Consideration of (7) shows that another (but equivalent) choice  
 of  $\varepsilon$  could have been made:  $\varepsilon = |J|$ . With this choice,  
 $x_3 = |J|^3$ , and the preceding relation reads:

$$\frac{|J|^{-4} Re^{-1/2}}{\pi} \int \frac{-A'}{\bar{x} - \xi} d\xi - p_2(\bar{x}, y \rightarrow 0) = -(|J|/J)A(\bar{x}).$$

This choice implies that we concentrate on thermal ef-  
 fects rather than on perfect fluid effects, if  $|J| \sim Re^{-1/8}$   
 (note that  $Re^{-1/8} \gg Re^{-1/2}$ ), the three terms are of the  
 same magnitude (as seen in the preceding paragraph).  
 Now, if  $|J| \gg Re^{-1/8}$  (or  $\tilde{J}$  bigger than one) there is no

315 interaction of the boundary layer with the external  
 316 perfect fluid, the thermal effect is dominant and the  
 317 pressure displacement relation degenerates in the form

$$p_2(\bar{x}, y \rightarrow 0) = \bar{p}(\bar{x}) = -A(\bar{x}) \quad (12)$$

319 for a cold wall ( $J < 0$ ), and in the form

$$p_2(\bar{x}, y \rightarrow 0) = \bar{p}(\bar{x}) = A(\bar{x}) \quad (13)$$

321 for a hot one ( $J > 0$ ), where in both cases  
 322  $Re^{-1/8} \ll |J| \ll 1$ . This shows that the upper deck is not  
 323 necessary for the interaction to take place (as noted by  
 324 Bowles [2]), the same phenomenon exists in free con-  
 325 vection hypersonic flows [5, 7, 26] for cold wall.

326 3.1.4. The fundamental problem of mixed convection on  
 327 “double deck” scales with displacement

328 Finally, the mechanism relevant for the problem of  
 329 infinitely small mixed convection is without external  
 330 perfect fluid retroaction, the whole process of interaction  
 331 takes place in the main deck. This is a double deck in-  
 332 teraction. We write here the final re-scaled problem (in  
 333 order to avoid  $U'_0(0)$ ). With scales

$$\begin{aligned} x &= L + |J|^3(L/U'_0(0))\tilde{x}, & y &= |J|((U'_0(0))^{-2}L/Re^{1/2})\tilde{y}, & t &= |J|^2(L/U_\infty)\tilde{t}, & u &= |J|((U'_0(0))^{-1}U_\infty)\tilde{u}, & v &= (|J|^{-1}((U'_0(0))^{-2}U_\infty Re^{-1/2}))\tilde{v}, & p &= J^2((U'_0(0))^{-2}\rho U_\infty^2)\tilde{p} \end{aligned}$$

335 (and  $Re^{-1/8} \ll |J| \ll 1$ ), the final “canonical problem of  
 336 infinitely small mixed convection” is

$$\frac{\partial}{\partial \tilde{x}} \tilde{u} + \frac{\partial}{\partial \tilde{y}} \tilde{v} = 0, \quad (14)$$

338

$$\frac{\partial}{\partial \tilde{t}} \tilde{u} + \tilde{u} \frac{\partial}{\partial \tilde{x}} \tilde{u} + \tilde{v} \frac{\partial}{\partial \tilde{y}} \tilde{u} = -\frac{d}{d\tilde{x}} \tilde{p} + \frac{\partial^2}{\partial \tilde{y}^2} \tilde{u}. \quad (15)$$

340 Boundary conditions are: no-slip at the wall ( $\tilde{u} = \tilde{v} = 0$   
 341 in  $\tilde{y} = 0$ ), no displacement far upstream ( $\tilde{A} = 0$  in  
 342  $\tilde{x} \rightarrow -\infty$ ), the matching  $\tilde{y} \rightarrow \infty, \tilde{u} \rightarrow \tilde{y} + \tilde{A}$  and the  
 343 coupling relation (hot wall,  $\text{sign}(J) = 1$ , cold wall  
 344  $\text{sign}(J) = -1$ )

$$\tilde{p} = \text{sign}(J)\tilde{A}. \quad (16)$$

346 The introduction of time changes only the lower deck by  
 347 the adjunction of the  $\partial \tilde{u} / \partial \tilde{t}$  term [34]. Fig. 3 displays a  
 348 rough sketch of the double deck structure.

349 3.1.5. Resolution

350 3.1.5.1. The eigenvalue solution. System (14)–(16) admits  
 351 the Blasius solution  $\tilde{u} = \tilde{y}$  as the basic one. Invariance by  
 352 translation in space and time suggests linearized solu-  
 353 tions of the form:

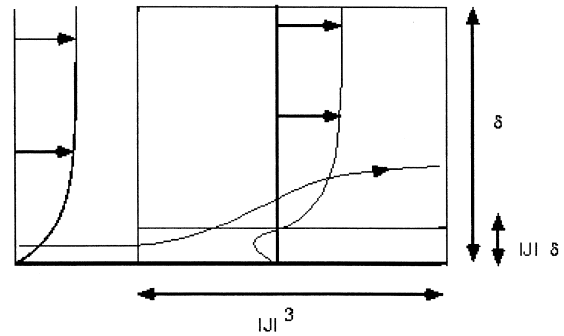


Fig. 3. The two final layers involved: the boundary layer itself and a thin wall layer.

$$\begin{aligned} \tilde{u} &= \tilde{y} + a e^{i(k\tilde{x} - \omega\tilde{t})} f'(\tilde{y}), & \tilde{v} &= -ika e^{i(k\tilde{x} - \omega\tilde{t})} f(\tilde{y}), \\ \tilde{p} &= a e^{i(k\tilde{x} - \omega\tilde{t})}, \end{aligned}$$

355 where  $a \ll 1$ . After substitution,  $f$  verifies an Airy dif-  
 356 ferential equation with the variable  $\eta = (ik)^{1/3} \tilde{y}$ , so  
 357 classically we find:

$$-f'(\infty) = \frac{(ik)^{1/3}}{Ai'(-i^{1/3} \omega/k^{2/3})} \int_{-i^{1/3} \omega/k^{2/3}}^{\infty} Ai(\zeta) d\zeta. \quad (17)$$

359 3.1.5.2. Cold wall, eigenvalue and comparison with  
 360 Steinrück. In the case of cold wall, the coupling ( $\tilde{p} = -\tilde{A}$ ) gives  $1 = -f'(\infty)$ , and a stationary exponen-  
 361 tially growing solution may be obtained:  $\omega = 0$ ,  
 362  $ik = \Lambda = (-3Ai'(0))^3 \simeq 0.47$ . We recover the same be-  
 363 havior as in hypersonic flows [7, 13], in the birth of  
 364 hydraulic jumps [3] and in supersonic pipe flows [27].  $\Lambda$   
 365 is called the Lighthill eigenvalue, it shows that there is  
 366 upstream influence, for example the preceding solution  
 367 is the linearization of what happens far upstream of the  
 368 separating point. The occurrence of eigen functions  
 369 states that system (2)–(5) is not parabolic.

370 We have proved that the perturbation grows like  
 371  $\exp[(-3Ai'(0))^3 \tilde{x}]$ . It may be compared with Steinrück's  
 372 result; he showed that the system (2)–(5) scaled longi-  
 373 tudinally by  $L_T$  admits near the origin eigen function  
 374 growing like  $\exp[(\lambda_0^+ / \xi_0^+) \tilde{\xi}]$ , where  $\lambda_0^+ = 2U'_0(0)$   
 375  $(-3Ai'(0))^3$ , ([37, formula 2.29] or [38, A.15], with  $Pr = 1$ ,  
 376  $U'_0(0) = f''(0) = 0.33321$  and  $\int_0^\infty Ai(\zeta) d\zeta = 1/3$  where  
 377  $\xi = (x/L_T)^{1/2}$  and where  $\xi_0$  is the place where the flow is  
 378 perturbed. If we substitute  $\lambda_0^+$ ,  $\xi$  and  $\xi_0$  in the expo-  
 379 nential, bearing in mind  $L/L_T = J^2$ , and  $|J| \ll 1$ , and  $\xi_0$   
 380 is  $(L/L_T)^{1/2}$  (i.e.  $|J|$ ), we rewrite it with our variables, and  
 381 develop with the first power of  $|J|$ :  
 382

$$\begin{aligned} e^{(\lambda_0^+ / \xi_0^+) \tilde{\xi}} &= \exp \left( \frac{\lambda_0^+}{|J|^3} (1 + |J|^3 (1/U'_0(0)) \tilde{x})^{1/2} \right) \\ &\sim \exp \left( |J|^{-3} \lambda_0^+ + \lambda_0^+ (1/U'_0(0)) \tilde{x}/2 \right). \end{aligned}$$

384 So, factorizing  $\exp(|J|^{-3}\lambda_0^+)$  and substituting the value of  
 385  $\tilde{\lambda}_0^+$ , we recover the exponential growth with  $\tilde{x}$ :

$$\exp(-3Ai'(0))^3 \tilde{x}.$$

387 So the conclusion is that the triple deck theory (which is  
 388 a theory in the limit of small  $J$  at  $x = 1$ ) is equivalent to  
 389 Steinrück's result (with only a different choice of scales:  
 390  $L_T$  instead of  $L$  so  $J = 1$  and  $x$  is small).

391 *3.1.5.3. Non-linear resolution of the fundamental problem.*

392 The stationary and non-linear self-induced solution with  
 393  $\tilde{p} = -\tilde{A}$  law is numerically computed and asymptotically  
 394 described in [13]. This solution is plotted in Fig. 4, we see  
 395 that the self-developing displacement  $-A$  is superposed  
 396 on to the pressure; the skin friction becomes negative.  
 397 The upstream pressure is in  $e^{0.4681x}$  while the downstream  
 398 is in  $0.94796x^{0.4305}$  (this last behavior is noticeable very  
 399 far downstream, at least  $x > 10^3$ ; these results are taken  
 400 from [13]). To compute this, we use a standard Keller  
 401 Box (with flare approximation) scheme for the lower  
 402 deck (adapted for the triple deck from [4]). This is an  
 403 inverse method which allows to catch separation:  $-\tilde{A}$  is  
 404 given and  $\tilde{p}$  is computed. A “verse method”, which is  
 405 iterative (details may be found in [22], and which has  
 406 been used in another hypersonic triple deck case by  
 407 Lagrée [18]) is used to couple the lower deck and the  
 408 pressure-deviation relation. It means that, given a dis-  
 409 placement  $-\tilde{A}^n$  at iteration level  $n$ , the next  $-\tilde{A}^{n+1}$  is  
 410 obtained as follows:

$$-\tilde{A}^{n+1} = -\tilde{A}^n + \lambda \left( \frac{dp^n}{dx} - \frac{d\tilde{p}^n}{dx} \right) + \mu(p^n - \tilde{p}^n),$$

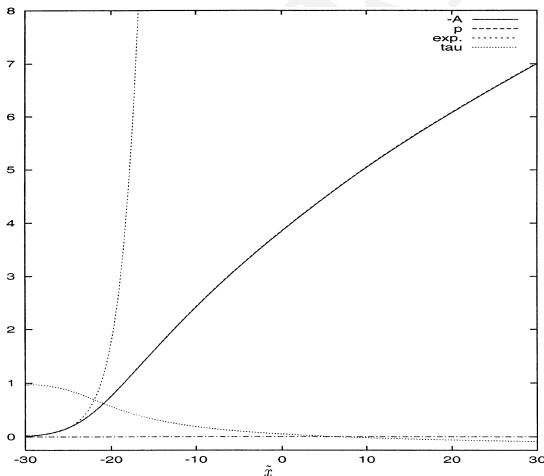


Fig. 4. Linearized eigen solution (“exp.” is  $\exp(-3Ai'(0))^3 \tilde{x}$ ), and non-linear solution of the self induced ( $\tilde{p} = -\tilde{A}$ ) problem solved with Keller Box and “semi-inverse” coupling: pressure ( $p$ ), displacement ( $-A$ ) and skin friction ( $\tau$ ).

where  $\tilde{p}^n$  is the lower deck Keller Box result associated  
 with  $-\tilde{A}^n$ ,  $p^n$  is the pressure associated with the dis-  
 placement  $-\tilde{A}^n$ , (here simply:  $p^n = -\tilde{A}^n$ , (16), with  $\lambda$  and  
 $\mu$  being relaxation coefficients. These coefficients are  
 chosen in order to stabilize the iterations: the complex  
 gain modulus is imposed to be smaller than one for all  
 spatial frequencies smaller than  $k_{\max} = \pi/\Delta x$  ( $\Delta x$  is the  
 longitudinal discretization step) and greater than  $\pi/L$  ( $L$   
 is the size of the computational domain). This gain may  
 be written exactly in the vicinity of the null solution  
 ( $p = -A = 0$  is a solution), in this case Eq. (17) gives for  
 the Fourier transform (FT) of pressure and displace-  
 ment small perturbations:

$$FT(\tilde{p}^n) = (ik^{1/3}) \frac{FT(-A^n)}{-3Ai'(0)},$$

while Eq. (16) gives  $FT(p^n) = FT(-\tilde{A}^n)$ , then with  
 $G = FT(-\tilde{A}^{n+1})/FT(-\tilde{A}^n)$ , we have:

$$G = 1 + (\lambda ik + \mu) \left( 1 - \left( \frac{(ik^{1/3})}{-3Ai'(0)} \right) \right).$$

The choice of the coefficients  $\lambda$  and  $\mu$  is such that, for  
 obvious reasons of stability,  $|G| < 1$  for all the spatial  
 frequencies present ( $\pi/L < k < \pi/\Delta x$ ). The non-linear  
 calculation is carried out with lower values for the said  
 coefficients. Here both ends are imposed: in  $x = -L/2$   
 and in  $x = L/2$ , the perturbation of  $-A$  is 0 at the first  
 step of the domain ( $-L/2$ ), and is imposed  $-A_m$  at the  
 output ( $L/2$ ).  $L = 60$  and  $-A_m = 7$  were largely sufficient  
 for our purpose. The Keller Box is a marching scheme:  
 $d\tilde{p}^n/dx$  is a backward derivative, the upstream influence  
 is recovered by the derivative of the pressure  $dp^n/dx$   
 which is a forward derivative.

*3.1.5.4. Hot wall instability.* The pressure displacement  
 relation  $\tilde{p} = \tilde{A}$  does not permit upstream influence, so  
 the flow is now really parabolic but unstable: the dis-  
 persion equation

$$\frac{(ik)^{1/3}}{Ai'(-i^{1/3}\omega/k^{2/3})} \int_{-i^{1/3}\omega/k^{2/3}}^{\infty} Ai(\xi) d\xi = 1$$

gives  $\omega = 2.3$  and  $k = 1.0$ . The scaled values for a neu-  
 tral Tollmien–Schlichting wave are then  $\omega^* = 2.3|J|^{-2}$   
 ( $U_0^*/L$ ), and  $\lambda^* = 18.9|J|^3 L$ .

*3.2. Bigger J with no displacement*

*3.2.1. New main deck*

The preceding structure is characterized by the inter-  
 action between the lower deck and the main deck by a  
 pressure–displacement function: the pressure in the  
 lower deck produces a displacement which changes the  
 pressure again in the main deck, and so on. Here in  
 discussing relation (8), we confine the interaction in the

457 lower deck itself, without retroaction in the main deck.  
 458 This idea is in fact deduced from Steinrück and from  
 459 Daniels [10]. The latter author has found the self-similar  
 460 solution  $U_0$ ,  $p_0$  and  $\theta_0$  associated to a problem with a  
 461 superposition of a jet and a constant flow with an adi-  
 462 abatic wall. Numerical explosions with a marching  
 463 scheme were observed which lead him to investigate the  
 464 corresponding eigenvalue problem for the said flow.

465 Up to now, pressure was found to be of the order of  
 466  $\varepsilon^2$ , while perturbations of  $u$  velocity component and  
 467 displacement  $-A$  in the main deck were found of order  $\varepsilon$ .  
 468 Similar interaction appears in pipe flows in the presence  
 469 of a bump, without thermal effect, (see [29,33]). The  
 470 bump gives rise to perturbation of pressure (of order  $\varepsilon^2$ )  
 471 with no displacement in the main deck (at order  $\varepsilon$ ):  
 472  $-A = 0$ . This  $O(\varepsilon^2)$  pressure drives perturbations in the  
 473 main deck of  $O(\varepsilon^2)$  in velocity, and so a  $O(\varepsilon^2)$  dis-  
 474 placement.

475 If now we introduce thermal effects and if  $J$  is small,  
 476 the conclusion is the same:  $-A = 0$  in the main deck at  
 477 order  $\varepsilon$ . Now if  $J$  becomes of order unity ( $J = O(\varepsilon^0)$ ),  
 478 relation (8) suggests that the perturbation of pressure is  
 479 of order  $\varepsilon$ . But, because of the  $O(\varepsilon)$  matching of veloc-  
 480 ities between lower and main deck, the pressure in the  
 481 lower deck is always of order  $\varepsilon^2$ . Thus the matching of  
 482 pressure implies again that there is no  $\varepsilon p_1$  contribution:  
 483 there is again no displacement  $\varepsilon A$  at first order (it is the  
 484 same as in the “double deck” structure pointed out be-  
 485 fore). With no anticipation, we put here  $\varepsilon^\alpha$  for the order  
 486 of the perturbations in this new deck, with  $\alpha > 1$  (the  
 487 complete analysis will show that the matching with the  
 488 lower deck will give surprisingly  $\alpha = 3/2$  and not 2 as in  
 489 pipe flows); here  $U_0$ ,  $p_0$  and  $\theta_0$  denote the solution (as  
 490 computed by Daniels) with  $x$  scaled by  $L_T$ , and  $y$  by  $\delta L_T$   
 491 (boundary layer thickness in  $L_T$  scales,  $Re$  is computed  
 492 with  $L_T$ ) that is perturbed. As the scale is  $L_T$ , in this  
 493 section  $J$  stands for  $\text{sign}(J)$ .

$$u = U_0(y) + \varepsilon^\alpha u_x, \quad v = \frac{\delta \varepsilon^\alpha}{x_3} v_x, \quad p = p_0 + \varepsilon^\alpha p_x,$$

$$\theta = \theta_0 + \varepsilon^\alpha \theta_x, \quad x = 1 + x_3 \hat{x}, \quad y = y.$$

495 As long as  $1 \gg \varepsilon \gg Re^{-1/6}$ , the main deck problem is  
 496 different because the longitudinal gradient of pressure is  
 497 still present:

$$\frac{\partial}{\partial \hat{x}} u_x + \frac{\partial}{\partial y} v_x = 0, \tag{18}$$

499

$$U_0(y) \frac{\partial}{\partial \hat{x}} u_x + v_x U_0'(y) = - \frac{\partial}{\partial \hat{x}} p_x, \tag{19}$$

501

$$0 = - \frac{\partial}{\partial y} p_x + J \theta_x, \tag{20}$$

503

$$U_0(y) \frac{\partial}{\partial \hat{x}} \theta_x + v_x \theta_0'(y) = 0, \tag{21}$$

where  $U_0(y)$  solves the mixed convection problem. If we  
 505 define  $\psi_x$  the perturbation of the stream function,  $\theta_x$  is  
 506 straightforward:  $\theta_x = \psi_x(\hat{x}, y) \theta_0'(y) / U_0(y)$ . After elimi-  
 507 nation of the velocities and pressure, we have to solve a  
 508 modified Rayleigh equation: 509

$$\frac{\partial^2}{\partial y^2} \psi_x - \left( \frac{U_0''(y)}{U_0(y)} - J \frac{\theta_0'(y)}{U_0^2(y)} \right) \psi_x = 0. \tag{22}$$

This equation may be solved in  $y$  in assuming zero  
 511 perturbation at the outer edge (for sake of simplicity we  
 512 suppose that there is no upper deck of perturbed perfect  
 513 fluid involving the Hilbert integral) and the matching for  
 514  $p_x$  in  $y = 0$  is discussed later. The value of  $u_x(\hat{x}, 0)$  will  
 515 not interfere with the lower deck. 516

If  $\delta \varepsilon^2 / x_3^2 = \varepsilon^2 / \delta$ , then the transverse velocity  $v_x$  is  
 517 present too in the transverse pressure gradient equation  
 518 (20), so it is now 519

$$U_0(y) \frac{\partial}{\partial \hat{x}} v_x = - \frac{\partial}{\partial y} p_x + J \theta_x;$$

the equation for  $\psi_x$  may be then obtained. If this term is  
 521 in the equations, then we have  $x_3 = \delta = Re^{-1/2}$  and  
 522  $\varepsilon = Re^{-1/6}$ , and the main deck has same scales in both  
 523 directions. 524

3.2.2. *New lower deck: the fundamental problem of mixed* 525  
*convection on “single deck” scales with no displacement* 526

For the sake of simplicity we put  $U_0'(0) = 1$  and  
 527  $|\theta_0'(0)| = 1$ . The lower deck problem is then changed by  
 528 the fact that the transverse pressure variation is within  
 529 the lower deck, (in Section 3.2.1, the transverse variation  
 530 of pressure took place in the main deck), it is a single  
 531 deck interaction: 532

$$u = \varepsilon \hat{u}, \quad v = \varepsilon^2 \hat{v}, \quad p = p_\infty + J \varepsilon \hat{y} + \varepsilon^2 \hat{p}_2,$$

$$\theta = 1 + \varepsilon \hat{\theta}, \quad x = 1 + \varepsilon^3 \hat{x}, \quad y = \varepsilon \hat{y},$$

(because  $x_3 = \varepsilon^3$ ), 534

$$\frac{\partial}{\partial \hat{x}} \hat{u} + \frac{\partial}{\partial \hat{y}} \hat{v} = 0, \tag{23}$$

536

$$\hat{u} \frac{\partial}{\partial \hat{x}} \hat{u} + \hat{v} \frac{\partial}{\partial \hat{y}} \hat{u} = - \frac{\partial}{\partial \hat{x}} \hat{p}_2 + \frac{\partial^2}{\partial \hat{y}^2} \hat{u}, \tag{24}$$

538

$$0 = - \frac{\partial}{\partial \hat{y}} \hat{p}_2 + J \hat{\theta}, \tag{25}$$

540

$$\hat{u} \frac{\partial}{\partial \hat{x}} \hat{\theta} + \hat{v} \frac{\partial}{\partial \hat{y}} \hat{\theta} = \frac{\partial^2}{\partial \hat{y}^2} \hat{\theta}. \tag{26}$$

542 The matching is  $\hat{u} \rightarrow \hat{y}$  and  $\hat{\theta} \rightarrow -\hat{y}$ , for  $\hat{y} \rightarrow \infty$ , because  
 543 there is no displacement. At the wall, the boundary  
 544 conditions are obvious:  $\hat{u} = \hat{v} = \hat{\theta} = 0$ . The pressure  
 545 matches at order  $\varepsilon^2$ , that is the value of the lower deck  
 546 pressure for  $\hat{y} \rightarrow \infty$  which makes the main deck develop,  
 547 and there is no retroaction from the main deck to the  
 548 lower one. All the problem lies in the lower deck: there is  
 549 no need for an external pressure change (because here  
 550  $\partial \hat{p}_2 / \partial \hat{y} \neq 0$ ). This is true for any  $\varepsilon$  in the range  
 551  $1 \gg \varepsilon \geq Re^{-1/6}$ .

552 3.2.3. Linearized resolution

553 Branching solutions are obtained from the linearized  
 554 system deduced from (23)–(26), where  $(u, v, p_2, \theta)$  de-  
 555 notes perturbations from the basic state  $(\hat{y}, 0, 0, 0, 0)$   
 556 (here  $J$  is  $\text{sign}(J)$ ):

$$\frac{\partial}{\partial \hat{x}} u + \frac{\partial}{\partial \hat{y}} v = 0, \tag{27}$$

558

$$\hat{y} \frac{\partial}{\partial \hat{x}} u + v = -\frac{\partial}{\partial \hat{x}} p_2 + \frac{\partial^2}{\partial \hat{y}^2} u, \tag{28}$$

560

$$0 = -\frac{\partial}{\partial \hat{y}} p_2 + J(\theta), \tag{29}$$

562

$$\hat{y} \frac{\partial}{\partial \hat{x}} \theta + v = \frac{\partial^2}{\partial \hat{y}^2} \theta. \tag{30}$$

564 This suggests looking for solutions in the form:

$$u = e^{\kappa \hat{x}} \phi'(\hat{y}), \quad v = -\kappa e^{\kappa \hat{x}} \phi(\hat{y}), \quad p_2 = J(g(\hat{y})) e^{\kappa \hat{x}},$$

$$\theta = e^{\kappa \hat{x}} g'(\hat{y}),$$

566 with the pressure value given at the wall (as the system is  
 567 linear we simply write  $g(0) = 1$ ).  $\kappa$  is the eigenvalue that  
 568 we are looking for. We note that the system may be  
 569 written as:

$$\left( \frac{\partial}{\partial \hat{y}} \frac{\partial}{\partial \hat{y}} - \kappa \hat{y} \right) g'(\hat{y}) = \kappa \phi(\hat{y}),$$

$$\left( \frac{\partial}{\partial \hat{y}} \frac{\partial}{\partial \hat{y}} - \kappa \hat{y} \right) \phi''(\hat{y}) = J \kappa g'(\hat{y}). \tag{31}$$

571 If we write  $\eta = \kappa^{1/3} \hat{y}$ , so that  $\kappa$  disappears from the  
 572 problem, any  $\kappa$  is convenient. The problem is solved  
 573 numerically for  $J = -1$  by a finite difference method  
 574 with time reintroduced to provide for a relaxation mean  
 575 of the numerical scheme. In Fig. 5, the computed ve-  
 576 locity profile  $\phi'(\eta)$  is compared with the corresponding  
 577 asymptotic solution while temperature results,  $g'(\eta)$ , are  
 578 shown in Fig. 6, (no solution was found with this  
 579 method for  $J = 1$ ). The profiles of velocity and tem-  
 580 perature slowly decrease in oscillating to 0 as  $\eta \rightarrow \infty$ .  
 581 This is coherent with the leading term of  $\phi$  which is in  $\eta^n$ ,

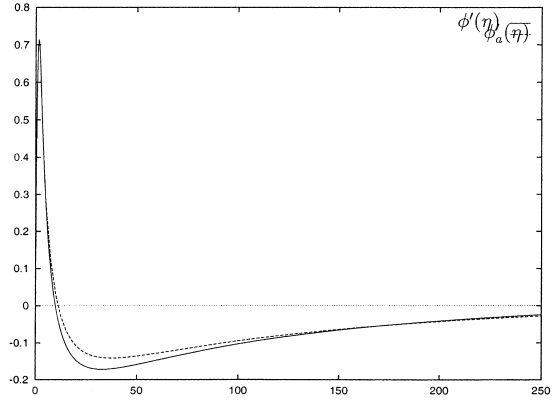


Fig. 5. Comparison of the computed value of  $\phi'(\eta)$  and asymptotic value

$$\phi'_a(\eta) = \frac{-(\sqrt{3} \cos(\frac{\sqrt{3} \log(\eta)}{2}))}{2\sqrt{\eta}} - \frac{\sin(\frac{\sqrt{3} \log(\eta)}{2})}{2\sqrt{\eta}}.$$

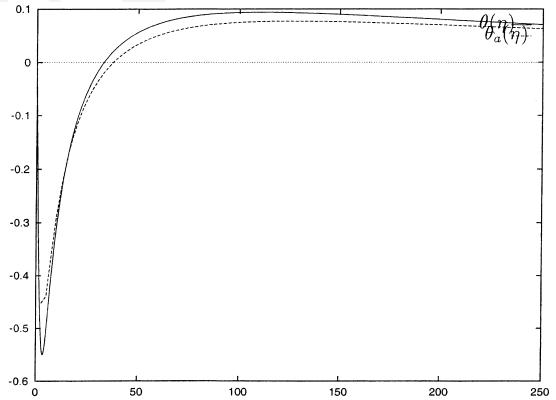


Fig. 6. Comparison of the computed value of  $\theta(\eta)$  and asymptotic value

$$\theta_a(\eta) = \frac{-(\sin(\frac{\sqrt{3} \log(\eta)}{2}))}{\sqrt{\eta}}.$$

582 where  $n$  solves  $n^2 - n + 1 = 0$ . Hence  $\phi$  involves  $\eta^{(1 \pm i\sqrt{3})/2}$   
 583 as  $\eta \rightarrow \infty$ , thereby implying that  $v$  is proportional to  
 584  $\sqrt{\eta} \sin(\sqrt{3} \log(\eta)/2)$ , and by consequence  $u$  becomes  
 585 proportional to  $-(d/d\eta)(\sqrt{\eta} \sin(\sqrt{3} \log(\eta)/2))$  and  $\theta$  to  
 586  $(-1/\sqrt{\eta}) \sin(\sqrt{3} \log(\eta)/2)$  (the exact coefficient of pro-  
 587 portionalities has not been determined).

588 Let us return now to the matching of the two layers in  
 589 order to obtain  $\alpha$ . In the lower deck the pressure is  $O(\varepsilon^2)$ ,  
 590 and behaves for large  $\hat{y}$  like  $\sqrt{\hat{y}}$ , so, written in outer  
 591 variables the pressure becomes  $\varepsilon^2 \sqrt{\hat{y}} \sim \varepsilon^{3/2} \sqrt{y}$ . In the  
 592 vicinity of  $y = 0$ , (22) behaves as



$$\frac{\partial^2}{\partial y^2} \psi_x + J \frac{1}{y^2} \psi_x \simeq 0.$$

594 If  $J = -1$ ,  $\psi_x$  involves the same powers of  $y$  as  $\eta$ :  
 595  $y^{(1 \pm i\sqrt{3})/2}$ , and hence  $\theta_x$  is proportional to combinations  
 596 of  $y^{(-1 \pm i\sqrt{3})/2}$  and the pressure (of order  $\varepsilon^2$ ) contains the  
 597 square root of  $y$ . Matching of the pressure between the  
 598 two decks leads to  $\alpha = 3/2$ . With perturbation of order  
 599  $\varepsilon^{3/2}$  the other matchings are straightforward. We con-  
 600 clude that any value of  $\kappa$  is acceptable and creates a self-  
 601 induced solution in the lower deck with no first-order  
 602 displacement: the dominant variations of velocities and  
 603 pressure are confined in the lower deck, the main deck is  
 604 passive.

### 605 3.2.4. Comparison with Daniels and Steinrück results

606 Daniels solves a set of equations closely related to the  
 607 preceding one, and without reference to triple deck. The  
 608 main difference is that he chooses non-linear profiles:  
 609  $U_0(y) \simeq y^{b-1}$  and  $\theta_0(y) \simeq \theta_0(0) + y^c$ , near  $y = 0$ . This  
 610 may be interpreted as a thicker lower deck (the matching  
 611 is not in the linear region but somewhere higher). So the  
 612 longitudinal scale is now  $x_3 = \varepsilon^{b+1}$ . The adiabaticity  
 613 gives in his study  $(-\partial/\partial \hat{y})p_2 = 0$ . He finds which exact  
 614 power  $b$  of  $\hat{y}$  is coherent for the lack of what we would  
 615 call the displacement function and that he calls “an orig-  
 616 in shift” in the transversal variable and noted as  $k_3(b)$ .  
 617 Thus he shows that  $k_3(b) = 0$  is necessary for the  
 618 matching of the two layers. As a result, near the singu-  
 619 larity, in  $\hat{x} < 0$ , the eigen function of the pressure is  
 620 found to be  $\simeq (-\hat{x})^{0.305}$  and there is a free interaction  
 621 with decreasing pressure.

622 Nevertheless, here we deal with  $b = 1$ ; instead of 0.305  
 623 we find  $1/3$ . We note that if  $b = 1$  in Daniels’s results,  
 624 there is no perturbation at all (see Fig. 4 in [10, p. 431],  
 625 where, when the pressure noted as  $q$  equals zero, the  
 626 displacement, noted as  $k_3(b)$ , equals zero as well); this is  
 627 the same here, if there is no transverse variation of  
 628 pressure, there is no possible linearized solution in the  
 629 lower deck with  $-A = 0$  except the null solution.

630 This solution is in fact what Steinrück calls the other  
 631 large eigenvalues, the oscillating behavior [37, Eq. (3.12)]  
 632 involves  $1/2 \pm i\sqrt{3}/4$  (it is the same because we took  
 633  $|\theta'_0(0)|/U'_0(0)^2 = 1$ ). So, the two sets of eigenvalues are  
 634 explained by a triple deck analysis.

## 635 4. Integral methods and branching solutions

### 636 4.1. Singularity

637 The preceding results for small  $J$  suggest that there is  
 638 no singularity in the equations, but because of non-pa-  
 639 rabolicity, a dependence with downstream conditions.  
 640 The flow may generate a self-induced interaction which  
 641 may lead to separation (at least in the  $\tilde{p} = -\tilde{A}$  case). So,

we may revisit the over-simplification of the problem  
 with integral methods as already mentioned by Schne-  
 ider and Wasel [32], to see whether we may go after the  
 singularity even in this very simple description. They  
 integrate over the whole boundary layer the system (2)–  
 (5) as follows:

$$\frac{d}{dx} \int_0^\infty \left[ u(1-u) + J \int_y^\infty \theta dY \right] dy = \left( \frac{\partial u}{\partial y} \right)_{y=0}.$$

This balance may be rewritten with the help of the dis-  
 placement function  $\delta_1$  (which is more physical in our  
 opinion):

$$\frac{d}{dx} \left[ \frac{\delta_1}{H} + JA\delta_1^2 \right] = \frac{f_2 H}{\delta_1}, \quad (32)$$

where  $H$  and  $f_2$  are standard notations [30];  $H = \delta_1/\delta_2$  is  
 by definition the shape factor, and  $f_2$  is defined from the  
 skin friction as  $f_2 = \delta_2(\partial u/\partial y)_{y=0}$ . Now the problem  
 must be solved with assumptions on the profile shape.  
 Classically  $f_2$  is a function of  $H$  and  $H$  is the function of  
 the pressure gradient and  $\delta_1$ . Like Schneider and Wasel,  
 we choose a simple sinusoidal profile with constant pa-  
 rameters ( $H = H_0$ ,  $A = A_0$  and  $f_2 = f_{20}$ ). The profile  
 $u = \sin(\pi(y/\delta))$  permits to evaluate  $H_0 = 2(2 - \pi)/$   
 $(\pi - 4)$  and  $f_{20} = 1 - \pi/4$ , the value of  $A_0$  is  
 $(-8 + \pi^2)/(2(-2 + \pi)^2)$ .

Then the integral equation (32) integrates in:

$$\left( \frac{1}{2}(\delta_1^2 - \delta_{10}^2) + \left( \frac{2}{3} \right) JH_0A_0(\delta_1^3 - \delta_{10}^3) \right) = f_{20}H_0^2(x - x_0).$$

At the leading edge  $x_0 = 0$  and  $\delta_{10} = 0$ , so we may ob-  
 tain an explicit  $\delta_1$  as a function  $x$ . It is much more simple  
 to plot  $(x(\delta_1), \delta_1)$  in a parametric mode. The case  $J = 0$   
 reduces of course to the approximation of the Blasius  
 solution:

$$\delta_{1B} = \sqrt{2f_2H_0^2}x^{1/2} = 1.742x^{1/2}$$

and for a non-zero negative  $J$  we find, with Schneider  
 and Wasel, that there is a singularity in the slope  
 $(d\delta_1/dx) = \infty$  in  $x_s = (24A_0^2H_0^4f_2J^2)^{-1}$ , where  $\delta_1 =$   
 $-1/(2A_0H_0J) = \delta_s$  say, which is finite.

### 4.2. Non-singular solution

Schneider and Wasel stopped with  $x_s$ , but we may  
 construct the sequel of the solution after  $x_s$  if we note  
 that for  $x > x_s$  the solution may be integrated if  $f_2 < 0$   
 (say  $f_2 = f_{2s}$ ). For the sake of oversimplification, we  
 only change the value of  $f_2$  in (32), the solution reads:

$$\left( \frac{1}{2}(\delta_1^2 - \delta_s^2) + \left( \frac{2}{3} \right) JH_0A_0(\delta_1^3 - \delta_s^3) \right) = f_{2s}H_0^2(x - x_s).$$

683 This expression is singular in  $x_s$  and valid for  $x > x_s$ . In  
 684 Fig. 7, we plot the two expressions of  $\delta_1$  (upstream and  
 685 downstream of  $x_s$ ) and  $\delta_{1B}$  on the same graph.

686 Thus we have a continuously varying  $\delta_1$  valid  
 687 throughout except in  $x_s$ . The displacement shows a  
 688 gradual increase as long as the thermal effect is small,  
 689 then it thickens in the vicinity of the separation, and  
 690 finally it slowly increases. We note that it looks like a  
 691 “jump” in the displacement thickness.

692 **4.3. Branching solutions**

693 Of course, a better description should involve a con-  
 694 tinuously varying  $H$  and  $f_2$  (this will enable to cross  $x_s$ ).  
 695 As a first step in this direction, we present an oversim-  
 696 plified argument – we may develop the shape factor  
 697 (only in the right-hand side, in the left-hand side it has  
 698 no real influence) near the Blasius value as follows:  
 699  $H = H_0 - Jh(d\delta_1/dx)$ . We may justify this postulate in  
 700 noticing that for a small adverse pressure gradient a  
 701 small growth of  $H$  is promoted (this is true in a classical  
 702 boundary layer such as the Falkner Skan’s one where  
 703  $H_0 \simeq 2.59$  and  $h \simeq 2.88 \dots$ ), but here the variation of  
 704 pressure through the boundary layer is more or less  
 705 proportional to  $J\delta_1$ ; this introduces a parameter  $h > 0$ .  
 706 With these crude assumptions and at first order in  $J$ , a  
 707 new term appears, proportional to the second derivative  
 708 of the displacement:

$$\frac{d}{dx} \left[ \frac{\delta_1}{H} \right] \simeq Jh \left[ \frac{\delta_1}{H_0^2} \right] \frac{d^2 \delta_1}{dx^2} + \frac{d}{dx} \left[ \frac{\delta_1}{H_0} \right];$$

710 so (32) is now

$$Jh \left[ \frac{\delta_1}{H_0^2} \right] \frac{d^2 \delta_1}{dx^2} + \left[ \frac{1}{H_0} + 2JA\delta_1 \right] \frac{d}{dx} \delta_1 \simeq \frac{f_2 H_0}{\delta_1}.$$

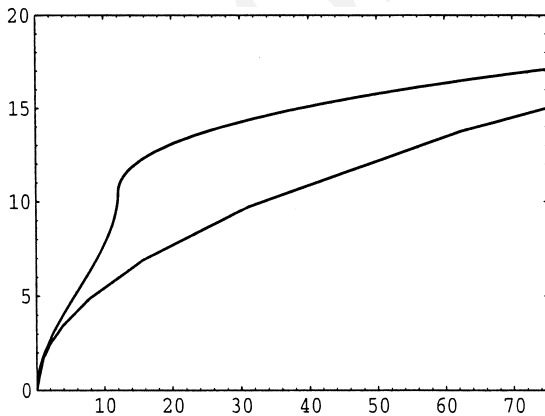


Fig. 7. The upper curve is the plot of  $\delta_1$  function of  $x$  as pre-  
 dicted by the very simple model, the lower one is the Blasius  
 solution.

With this ad hoc term in the equation, first, the singu-  
 larity will be smoothed (for example, we may construct  
 an asymptotic description of the equation in introducing  
 a region in  $x_s$  where  $(d^2\delta_1/dx^2)$  is not negligible...), and  
 second, closely linked eigen function may be exhibited if  
 we write  $\delta_1 = \delta_{10}(1 - ae^{Kx})$ , where  $\delta_{10}$  is the Blasius so-  
 lution frozen ( $K$  must be big) and  $K$  solves

$$hJ \left[ \frac{\delta_{10}}{H_0^2} \right] K^2 + K \left( \frac{1}{H_0} + 2JA\delta_{10} \right) + \frac{f_2 H_0}{\delta_{10}} \simeq 0.$$

The roots, for small  $J$  are at first order  $-(f_2 H_0^2)/\delta_{10}$  and  
 $(-J)^{-1}(H_0/h\delta_{10})$ . If  $J$  is positive, they are negative, so  
 any perturbation is damped, and the parabolic nature of  
 the flow is recovered. If  $J$  is negative, the first one re-  
 mains negative, but the other is positive and big leading to  
 a growing exponential on a short scale. This solution  
 destroys the parabolicity of the flow, and is clearly a  
 consequence of the  $h$  term. This behavior, qualitatively  
 similar to the complete resolution (as we will see in the  
 next paragraph) and with the occurrence of branching  
 exponential solutions (as in triple deck), shows again  
 how powerful the integral methods are [22] if the vari-  
 ation of  $H$  with the pressure gradient is not omitted. In  
 the next section, we look at how the previous results may  
 be observed on a complete numerical simulation of the  
 equations, and whether it is possible to obtain a sepa-  
 rated flow.

**5. Numerical computations**

**5.1. The problem**

As shown in the previous paragraph with different  
 scales and methods, solving the equations with a  
 marching scheme in  $x$  (stationary in  $t$ ) leads to the se-  
 lection of the eigenvalues and to a self-induced interac-  
 tion. In supersonic flows, the way to prevent this fact is  
 to construct an iterative coupled method as already  
 mentioned. It permits to impose boundary conditions at  
 both ends of the domain. Here the problem is that the  
 pressure changes across the boundary layer, so these  
 powerful methods are not applicable. We propose to  
 change the problem and to make it unsteady.

We have to solve (2)–(5) with the  $\partial_t$  term and new  
 boundary conditions at  $t = 0$  and at  $x \rightarrow \infty$ :

$$\frac{\partial}{\partial x} u + \frac{\partial}{\partial y} v = 0, \tag{33}$$

$$\frac{\partial}{\partial t} u + u \frac{\partial}{\partial x} u + v \frac{\partial}{\partial y} u = - \frac{\partial}{\partial x} p + \frac{\partial}{\partial y} \frac{\partial}{\partial y} u, \tag{34}$$

712  
713  
714  
715  
716  
717  
718  
  
720  
721  
722  
723  
724  
725  
726  
727  
728  
729  
730  
731  
732  
733  
734  
735  
736  
  
737  
738  
  
739  
740  
741  
742  
743  
744  
745  
746  
747  
748  
749  
750  
751  
  
753  
  
755

$$0 = -\frac{\partial}{\partial y} p + J\theta, \tag{35}$$

$$\frac{\partial}{\partial t} \theta + u \frac{\partial}{\partial x} \theta + v \frac{\partial}{\partial y} \theta = \frac{\partial}{\partial y} \frac{\partial}{\partial y} \theta, \tag{36}$$

with, at time  $t = 0$ :

$$\begin{aligned} u(x, y > 0, t = 0) &= 1, & u(x, y = 0, t = 0) &= 0, \\ v(x, y \geq 0, t = 0) &= 0, & \theta(x, y > 0, t = 0) &= 0, \\ p(x, y \geq 0, t = 0) &= 0, \end{aligned}$$

and after, for  $t > 0$ :

$$\begin{aligned} u(x, y = 0, t \geq 0) &= 0 & v(x, y = 0, t \geq 0) &= 0, \\ u(x, y \rightarrow \infty, t \geq 0) &= 1, & \theta(x, y = 0, t \geq 0) &= 1, \\ \theta(x, y \rightarrow \infty, t \geq 0) &= 0, & p(x, y \rightarrow \infty, t \geq 0) &= 0, \end{aligned}$$

$$\forall y, \text{ for } x > t, x \rightarrow \infty : \frac{\partial}{\partial x} u = 0, \quad \frac{\partial}{\partial x} v = 0, \quad \frac{\partial}{\partial x} p = 0, \\ \frac{\partial}{\partial x} \theta = 0.$$

If, at a given  $x$ , we wait for a long time, and with a big enough domain, we expect to find a steady solution which solves (2)–(5) too after a transient spreading.

### 5.2. Numerical discretization

The set of (33)–(36) is discretized in finite differences in the most simple way, second order in space  $x$ ,  $y$  and in time  $t$ . It is implicit in  $y$  and explicit in  $x$ . We introduce an internal loop to improve the description of the non-linear terms put as explicit source terms.

The first difficulty is now at the entry: we cannot begin the calculation in  $x = 0$  because the equations are singular at the origin, so we impose the Blasius boundary layer profile at any time  $t > 0$ , in  $x = x_{in} > 0$ . This creates a small non-dangerous perturbation.

The second one is at the exit, where  $x = x_{out}$ . The annulation of longitudinal derivatives ( $\partial/\partial x = 0$ ) at the outlet is a coherent boundary condition as long as no information has propagated (at velocity 1) from the nose. If  $t > x_{out}$ , it is not true anymore.

The third difficulty is the numerical discretization in  $x$ . If we put a centered derivative ( $(f_{i+1j}^N - f_{i-1j}^N)/2\Delta x$ ) we observe oscillations; by inspection, if we choose a downstream derivative ( $(3f_{ij}^N - 4f_{i-1j}^N + f_{i-2j}^N)/2\Delta x$ ) in the transport equations but we center  $v_{ij}^{N+1} = -((\psi_{i+1j}^{N+1} - \psi_{i-1j}^{N+1})/2\Delta x)$  in the incompressibility, no oscillations are observed and the back flow region is computed.

## 6. Results

### 6.1. Test cases

As a test case of our numerical discretization (for the unsteady part as well for the non-linear part), we have recomputed the classical problem of the starting flat plate (solved analytically by Stewartson [39,42] and numerically by Hall [15]).

For the sake of validation of boundary layer separation phenomena, we have computed the starting flow around a cylinder. We recover the Van Dommeln and Shen [45] result of finite time singularity. For this severe test, the three different discretizations in  $x$  were tested. We conclude that the effect of the choice of the longitudinal derivative (centered or not) on the position of the separating point is very small: a difference of 0.3%. In [21] we discuss more precisely those examples. Of course, this finite difference scheme in Eulerian description does not go near the singularity as Cassel et al. [8] do with boundary layer equations written in Lagrangian description. Nevertheless, it predicts the singularity, so this is an element of validation of the back flow calculation.

Next, we introduce the transverse buoyancy, but we impose the temperature to be  $x^{-1/2}$  rather than 1. For example if  $J = -0.025$  we obtain  $\delta_1 \simeq 1.9x^{1/2}$  and  $\partial u/\partial y(x, 0) \simeq 0.29x^{-1/2}$ ; the value  $\partial u/\partial y(x, 0)\sqrt{x}$  as a function of  $|J|\sqrt{x}$  for different time steps is plotted in Fig. 8 (the choice of abscissa  $\xi = |J|\sqrt{x}$  and ordinate  $f''(\xi, 0) = \partial u/\partial y(x, 0)\sqrt{x}$  comes from Steinrück's work based on self-similar variables).

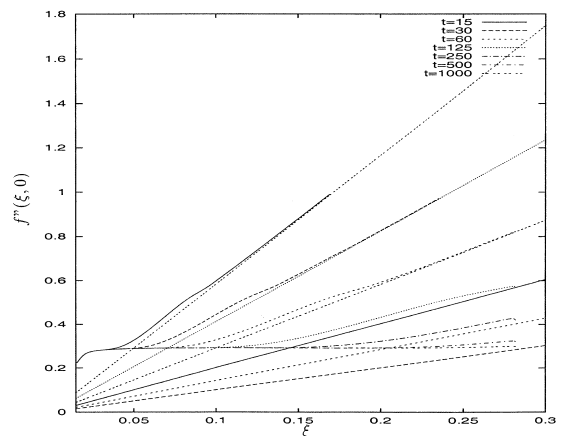


Fig. 8. Numerical computation of the reduced skin friction function as a function of the reduced longitudinal variable at different times (from  $t = 15$  to 3000) and in the case of wall temperature  $T_w(x) = 1/\sqrt{x}$ . The reduced Rayleigh skin friction is plotted as well (lines at time  $t = 15, 30, 60, 125, 250, 500$  and 1000. The final value is the self-similar one: 0.29).

822 The lines correspond to the Rayleigh solution of the  
 823 problem: an infinite flat plate impulsively moved and  
 824 heated. In this case  $(\sqrt{x}(\partial u/\partial y))(x, y = 0) = -1\sqrt{\pi x/t}$ ,  
 825 which is linear in  $|J|\sqrt{x}$  and whose slope decreases with  
 826 time  $t$ , they are plotted for comparison (so we see the  
 827 propagation of the influence of the nose). We note that it  
 828 takes a long time to obtain the stationary (here self-  
 829 similar) solution computed by Schneider [31] and Afzal  
 830 and Hussain [1], this flow is a particular case of the  
 831 generalized Falkner Skan mixed convection as pointed  
 832 out by Ridha [28]. The last points present a small discrepancy  
 833 because of the output effect: the upstream influence of  $(\partial/\partial x)p = 0$ .

835 This is an element for the validation of the thermal  
 836 coupling part of our discretization. Note, that for  
 837  $-0.8 \simeq J < 0$  there are two self-similar solutions, one  
 838 with a positive skin friction and an other with a negative  
 839 skin friction [28, 38]. Steinr uck [38] showed that it is  
 840 possible, near the critical value, to branch from the self-  
 841 similar flow (for  $x \rightarrow 0$ ) with positive skin friction to the  
 842 other, with negative skin friction (at large  $x$ ).

843 6.2. Starting flow, buoyant, non-self-similar results

844 In the sequel, we fix  $J = -0.025$ . The temperature of  
 845 the wall is equal to 1. This value of  $J$  is a compromise  
 846 between two effects: first, if  $J$  is too large, the interaction  
 847 takes place near the nose where the gradients are big,  $\Delta x$   
 848 must be not too small and  $x_{in}$  must also be not too small;  
 849 second, if  $J$  is too small, the Blasius part is well solved,  
 850 but the size of the computational domain is now too big.  
 851  $J = -0.025$  seems to be good enough to prevent those  
 852 two drawbacks.

853 In Fig. 9, we display the converged reduced skin  
 854 friction at the wall as function of the size of the domain

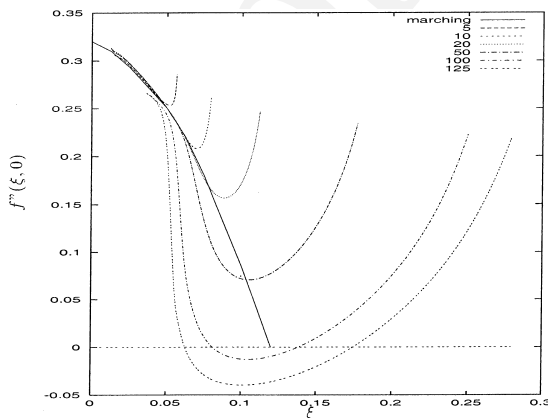


Fig. 9. The reduced skin friction function of the domain size. Results are compared with the calculation of Wickern (1991) (compiled by Steinr uck) and referred as marching. The size of the domain is  $x_{out} = 5, 10, 20, 50, 100$  and  $125$ .

(i.e. the value of  $x_{out}$ ). We note that, depending on this  
 size, we obtain different solutions. The first points present  
 an error coming from the discretization at the input, they  
 are not far from  $f''_{Blasius}(0) = 0.33$ . Reducing the step  
 size decreases this error (the error is amplified on the  
 graph because of the  $\sqrt{x}$  term coming from  $\xi = |J|\sqrt{x}$ ).  
 The quantity  $f''(\xi, 0) = (\partial u/\partial y)(x, 0)\sqrt{x}$  decreases to  
 a minimum and increases greatly after and reaches a  
 maximum at the end of the computational zone. This  
 minimum decreases as the size of the domain increases  
 and ultimately this leads to separation. Finally, we may  
 compare favorably results from Fig. 9 and Steinr uck's  
 results [37, p. 261, Fig. 1] reproduced in Fig. 2: most of  
 the curves have common parts with Wickern results  
 compiled by Steinr uck. But here the originality of our  
 work is that we catch the back flow, so our curves do not  
 stop at separation.

In Fig. 10, we plot the displacement thickness as a  
 function of  $x$  (final state) for the different domain sizes  
 compared with Blasius solution. Fig. 11 is a zoom of the  
 same figure showing the sudden increase of displacement  
 thickness associated to the boundary layer separation.

We do not observe any singularity at a finite time as  
 observed in all the boundary layer calculation for impulsive  
 flow [45]. In investigating smaller grid effects, we do not  
 observe oscillations as predicted by Cowley et al. [9] or  
 Smith and Elliot [36].

7. Conclusion

This problem is very interesting because it summarizes  
 all the difficulties of boundary layer flows: the existence  
 of eigen function destroying the parabolicity, boundary  
 conditions difficult to settle, occurrence of a back flow,  
 and numerical and physical instabilities.

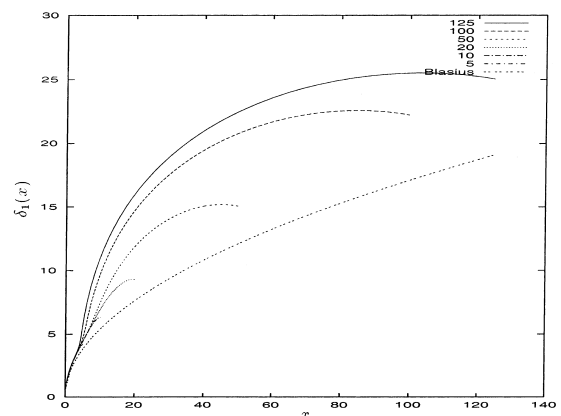


Fig. 10. The displacement thickness  $\delta_1(x)$  for several domain sizes ( $x_{out} = 5, 10, 20, 50, 100$  and  $125$ ).

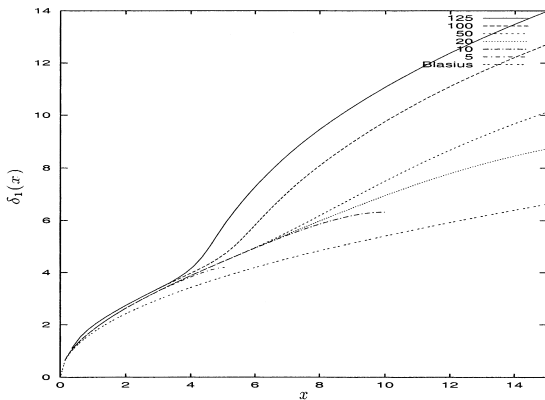


Fig. 11. The displacement thickness  $\delta_1(x)$  for several domain size, from the nose to  $x = 15$ .

888 Numerical calculations with marching techniques  
 889 have clearly shown [37] that there is a singularity in the  
 890 self-interaction of the boundary layer for  $J = O(1)$ . This  
 891 singularity is similar to the “branching solutions” obtained  
 892 in supersonic inviscid–viscous interacting flows  
 893 (and presented by Werle et al. [46]). These interacting  
 894 boundary layer flows were often solved with integral  
 895 methods, and we have presented here such a simplified  
 896 resolution too. The divergence of the numerical solution  
 897 was observed, and often explained with those integral  
 898 methods [22]. As we have exactly the same behavior as  
 899 clearly stated by Steinrück who compares a lot of numerical  
 900 results, we have presented here the same arguments: we  
 901 have showed that integral methods may be extended to  
 902 remove the singularity (as in aerodynamics), we have  
 903 showed that this behavior is natural from the triple deck  
 904 theory (in aerodynamics, the supersonic and hypersonic  
 905 boundary layer flows were the problems which have led  
 906 Neiland and Stewartson to introduce the triple deck  
 907 analysis).

908 Two different asymptotic structures were presented,  
 909 the first with small  $J$  predicts that there is no singularity  
 910 but amplification of any perturbation; the second at  $J$   
 911 of the order of one predicts a self-similar singularity at  
 912 any location. These two structures were shown to be those  
 913 found by Steinrück but with a different approach. Moreover,  
 914 we have presented a numerical computation showing that  
 915 the self-induced singularity may be removed if downstream  
 916 conditions are supplied (coherent with the first mechanism:  
 917 amplification of any perturbation at small  $J$ ). No general  
 918 physical boundary conditions were imposed, nevertheless  
 919 with a zero gradient output condition, we showed that  
 920 depending upon the size of the domain a different  
 921 branching solution may be selected. The boundary layer  
 922 may then separate and present a region of back flow  
 923 (even after step size reduction, no oscillations were  
 924 observed). This is a generalization of Steinrück results.

926 Some questions may arise, first of physical interpretation:  
 927 does this upstream influence describe the phenomenon of  
 928 “blocking” which is observed in stratified flows? Is it the  
 929 result of the existence of a kind of hydraulic internal jump?  
 930 This is possible because the hydraulic jump equation solved  
 931 by Higuera [16] is nearly the same as it involves a change  
 932 of pressure associated with the change of the thickness of  
 933 the film (analogous to  $\delta_1$ ), the inverse of the Froude  
 934 number being the analog of the buoyancy parameter; furthermore,  
 935 Higuera [17] solves the problem of a buoyant wall jet over  
 936 a finite plate with a singularity imposed at the end. His  
 937 work enters in greater details (influence of adiabatic wall  
 938 and of  $Pr$  number); there is a separation and a back flow  
 939 as well. The case of cold jet on adiabatic plate leads to  
 940 separation too; he compares qualitatively this result with  
 941 what happens in cavity-driven flow where a sort of  
 942 “hydraulic jump” is observed. Is it nearly impossible to  
 943 reach the location where  $J \simeq -1$  (incidentally, linear  
 944 stability of the  $J \simeq 1$  should be investigated) because  
 945 branching solutions have appeared far upstream of this  
 946 point where  $J \ll 1$ ? What are the real downstream  
 947 boundary conditions? Is it possible to find a set of those  
 948 boundary conditions which leads to a solution with a  
 949 region of back flow developing continuously downstream  
 950 (as proposed by Steinrück in self-similar flows)? 951

8. Uncited references

[14,23,40].

References

[1] N. Afzal, T. Hussain, Mixed convection over a horizontal plate, *J. Heat transfer* 106 (1984) 240–241.  
 [2] R.I. Bowles, 1994, private communication.  
 [3] R.I. Bowles, F.T. Smith, The standing hydraulic jump: theory, computations and comparisons with experiments, *J. Fluid Mech.* 242 (1992) 145–168.  
 [4] P. Bradshaw, T. Cebecci, J.H. Whitelaw, *Engineering calculation methods for turbulent flow*, Academic Press, New York, 1981.  
 [5] S.N. Brown, H.K. Cheng Lee, Inviscid viscous interaction on triple deck scales in a hypersonic flow with strong wall cooling, *J. Fluid Mech.* 220 (1990) 307–309.  
 [6] S.N. Brown, K. Stewartson, P.G. Williams, A non uniqueness of the hypersonic boundary layer, *Q. J. appl. Math.* 28, Pt1 (1975) 75–90.  
 [7] S.N. Brown, K. Stewartson, P.G. Williams, Hypersonic self induced separation, *Phys. Fluids* 18 (6) (1975).  
 [8] K.W. Cassel, F.T. Smith, J.D.A. Walker, The onset of instability in unsteady boundary-layer separation, *J. Fluid Mech.* 315 (1996) 223–256.  
 [9] S.J. Cowley, L.M. Hocking, O.R. Tutty, The stability of the classical unsteady boundary layer equation, *Phys. Fluids* 28 (2) (1985).

- 978 [10] P.G. Daniels, A singularity in thermal boundary-layer flow  
979 on a horizontal surface, *J. Fluid Mech.* 242 (1992) 419–440.
- 980 [11] P.G. Daniels, R.J. Gargaro, Buoyancy effects in stably  
981 stratified horizontal boundary-layer flow, *J. Fluid Mech.*  
982 250 (1993) 233–251.
- 983 [12] M. El Hafî, Analyse asymptotique et raccordements, étude  
984 d'une couche limite de convection naturelle, thèse de  
985 l'Université de Toulouse, 1994.
- 986 [13] J. Gajjar, F.T. Smith, On hypersonic self induced separa-  
987 tion, hydraulic jumps and boundary layer with algebraic  
988 growth, *Mathematika* 30 (1983) 77–93.
- 989 [14] W.N. Gill, D.W. Zeh, E. del Casal, Free convection on a  
990 horizontal plate, *ZAMP* 16 (1965) 359–541.
- 991 [15] M.G. Hall, The boundary layer over an impulsively started  
992 flat plate, *Proc. Roy. Soc. A* (1969) 401–414.
- 993 [16] F.J. Higuera, The hydraulic jump in a viscous laminar  
994 flow, *J. Fluid Mech.* 274 (1994) 62–92.
- 995 [17] F.J. Higuera, Opposing mixed convection flow in a wall jet  
996 over a horizontal plate, *J. Fluid Mech.* 342 (1997) 355–375.
- 997 [18] P.-Y. Lagrée, Influence of the entropy layer on viscous  
998 triple deck hypersonic scales, in: *Proceedings of the*  
999 *IUTAM symposium, Aerothermochemistry of spacecraft*  
1000 *and associated hypersonic flows, Marseille, France, 1–4*  
1001 *September 1992*, pp. 358–361.
- 1002 [19] P.-Y. Lagrée, Convection thermique mixte à faible nombre  
1003 de Richardson dans le cadre de la triple couche, *C.R. Acad.*  
1004 *Sci. Paris t. 318, Série II* (1994) 1167–1173.
- 1005 [20] P.-Y. Lagrée, Upstream influence in mixed convection at  
1006 small Richardson Number on triple, double and single  
1007 deck scales, in: Bois, Dériat, Gatignol, Rigolot (Eds.),  
1008 *Symposium on Asymptotic Modelling in Fluid Mechanics,*  
1009 *Lecture Notes in Physics, Springer, 1995*, pp. 229–238.
- 1010 [21] P.-Y. Lagrée, Résolution des équations de couche limite  
1011 interactive instationnaire et applications, Report  
1012 D.S.P.T.8, février 97, 1997.
- 1013 [22] J.-C. Le Balleur, Viscid- inviscid coupling calculations for  
1014 two and three- dimensional flows, Von Kármán Institute  
1015 for Fluid Dynamics, *Comput. Fluid Dynamics Lecture Ser.*  
1016 (1982) 04.
- 1017 [23] M.A. Lévêque, Les lois de transmission de la chaleur par  
1018 convection, *Ann. Mines Paris* 13 (1928) 201–409.
- 1019 [24] F. Méndez, C. Treviño, A. Liñán, Boundary layer separa-  
1020 tion by a step in surface temperature, *J. Heat Mass*  
1021 *Transfer* 35 (1992) 2725–2738.
- 1022 [25] V. Ya Neiland, Propagation of perturbation upstream with  
1023 interaction between a hypersonic flow and a boundary  
1024 layer, *Mekh. Zhid. Gaz.* 4 (1969) 53–57.
- 1025 [26] V. Ja Neiland, Some features of the transcritical boundary  
1026 layer interaction and separation, in: Smith, Brow (Eds.),  
1027 *IUTAM symposium: Boundary Layer separation, Spring-*  
1028 *er, 1986*, pp. 271–293.
- 1029 [27] A.I. Ruban, S.N. Timoshin, Propagation of perturbations  
1030 in the boundary layer on the walls of a flat chanel, *Fluid*  
1031 *Dynamics* (2) (1986) 74–79.
- [28] A. Ridha, Aiding flows non-unique similarity solutions of  
mixed-convection boundary-layer equations, *Z. Math.*  
*Phys.* 47 (1996) 341–352.
- [29] S. Saintlos, J. Mauss, Asymptotic modelling for separating  
boundary layers in a channel, *Int. J. Eng. Sci.* 34 (2) (1996)  
201–211.
- [30] H. Schlichting, *Boundary Layer Theory*, seventh ed.,  
McGraw-Hill, New York, 1987.
- [31] W. Schneider, A similarity solution for combined forced  
and free convection flow over a horizontal plate, *Int. J.*  
*Heat Mass Transfer* 22 (1978) 1401–1406.
- [32] W. Schneider, M.G. Wasel, Breakdown of the boundary  
layer approximation for mixed convection above an  
horizontal plate, *Int. J. Heat Mass Transfer* 28 (12)  
(1985) 2307–2313.
- [33] F.T. Smith, Flow through constricted or dilated pipes and  
channels, parts 1 and 2, *Q. J. Mech. Appl. Math.* 29 (1976)  
343–364.
- [34] F.T. Smith, On the non parallel flow stability of the Blasius  
boundary layer, *Proc. Roy. Soc. Lond. A* 366 (1979) 91–  
109.
- [35] F.T. Smith, On the high Reynolds number theory of  
laminar flows, *IMA J. Appl. Math.* 28 (1982) 207–281.
- [36] F.T. Smith, J.W. Elliot, On the abrupt turbulent reattach-  
ment downstream of leading-edge laminar separation,  
*Proc. Roy. Soc. Lond. A* 401 (1985) 1–27.
- [37] H. Steinrück, Mixed convection over a cooled horizontal  
plate: non-uniqueness and numerical instabilities of the  
boundary layer equations, *J. Fluid Mech.* 278 (1994) 251–  
265.
- [38] H. Steinrück, Mixed convection over a horizontal plate:  
self similar and connecting boundary-layer flows, *Fluid*  
*Dynamic Res.* 15 (1995) 113–127.
- [39] K. Stewartson, On the impulsive motion of a flat plate in a  
viscous fluid. II, *Q. J. Mech. Appl. Math.* 26 Pt2 (1951)  
143–152.
- [40] K. Stewartson, On the free convection from a horizontal  
plate, *ZAMP* 9a (1958) 276–282.
- [41] K. Stewartson, The theory of laminar boundary layers in  
compressible fluids, *Oxford Math. Monograph* (1964).
- [42] K. Stewartson, On the impulsive motion of a flat plate in a  
viscous fluid, *Q. J. Mech Appl. Math.* 4 Pt2 (1973) 183–  
198.
- [43] K. Stewartson, P.G. Williams, Self-induced separation,  
*Proc. Roy. Soc. A* 312 (1969) 181–206.
- [44] R.I. Sykes, Stratification effects in boundary layer flows  
over hills, *Proc. Roy. Soc. Lond. A* 361 (1978) 225–243.
- [45] L. Van Dommeln, S.F. Shen, The spontaneous generation  
of the singularity in a separating boundary layer, *J. Comp.*  
*Phys.* 38 (1980) 125–140.
- [46] M.J. Werle, D.L. Dwoyera, W.L. Hankey, Initial condi-  
tions for the hypersonic-shock/boundary-layer interaction  
problem, *AIAA J.* 11 (4) (1973) 525–530.